

# Triplet Energy Migration in Layer-by-Layer Deposited Ultrathin Polymer Films Bearing Tris(2,2'-bipyridine)ruthenium(II) Moieties

Toshiki Fushimi, Akimichi Oda, Hideo Ohkita, and Shinzaburo Ito\*

Department of Polymer Chemistry, Graduate School of Engineering, Kyoto University, Katsura, Nishikyo, Kyoto 615-8510, Japan

Received: June 30, 2004; In Final Form: September 28, 2004

Ultrathin polymer films bearing tris(2,2'-bipyridine)ruthenium(II) (Ru) moieties were fabricated by the layer-by-layer deposition technique. The triplet energy migration among the Ru moieties was investigated by emission spectroscopy for quenching of the phosphorescence of the Ru moiety by a ferrocene moiety in heterostructured layer-by-layer films. The absorbance of the Ru moiety in the films increased linearly as the number of bilayers increased, showing a linear growth of the thickness in a scale of nanometers. The quenching efficiency increased as the concentration of the Ru moiety increased. This increase in the efficiency showed that the triplet excitation energy migrates in the Ru layers. The diffusion of the excitation energy was analyzed quantitatively on the basis of one-dimensional diffusion in a finite thickness. A diffusion coefficient of  $2 \times 10^{-5} \text{ cm}^2 \text{ s}^{-1}$  was observed in the layer-by-layer films made of a polycation with 18 mol % of Ru moiety. The root mean square of the migration distance was calculated to be 36 nm, which is much longer than a Perrin radius of 1.5 nm for the direct quenching of the Ru moiety by the ferrocene moiety and comparable to that in singlet energy migration. This efficient triplet energy migration shows that the layer-by-layer films serve as a light-harvesting system.

## Introduction

Ultrathin films bearing chromophoric or redox moieties are attractive systems where elementary processes are well controlled because of the designed multilayered structures.<sup>1–11</sup> Spatial arrangement of these moieties with nanometer-scale precision is required to design and control energy transfer or charge transport.<sup>1–8</sup> Langmuir–Blodgett films<sup>1–9</sup> and self-assembled monolayers<sup>10,11</sup> have been used to aim at mimicking the system of photosynthesis. Miyashita et al. reported LB films bearing tris(2,2'-bipyridine)ruthenium(II) (Ru) moieties,<sup>8,9</sup> a promising dye with strong absorption in the visible region, redox activity, and remarkable photochemical stability.<sup>12</sup> However, there is a critical problem in systems fabricated on flat substrates. The problem is the low optical density of chromophores in ultrathin films because the thinness of active layers results in a limited number of effective chromophores per unit area. One approach toward obtaining a high optical density is deposition of materials on a porous substrate with a large surface area, which will greatly increase the load of chromophores. This strategy has brought big success in dye-sensitized solar cells where the surface concentration of dye deposited on porous  $\text{TiO}_2$  is about  $10^3$  times higher than that of systems on flat substrates.<sup>13</sup> Another approach is light-harvesting with antenna molecules, as seen in photosynthetic systems. Excitation energy migration<sup>14–17</sup> enables many chromophores far from an active interface also to participate in light-harvesting.<sup>17</sup> Combination of these approaches would be effective to fabricate highly efficient light-harvesting systems. The layer-by-layer films containing chromophoric units provide one of the possible molecular assemblies for this end.

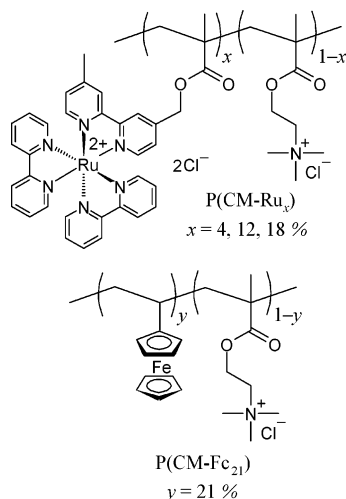
The layer-by-layer deposition technique developed by Decher et al. in 1991<sup>18,19</sup> is a suitable method for deposition of ultrathin films on flat and also on porous substrates. The method is extremely versatile because one can use not only polymers<sup>18–30</sup> but also charged nanoparticles such as molecular aggregates, nanoclusters, and colloidal particles.<sup>19,31–33</sup> There are extensive studies on the fabrication of films consisting of conducting polymers,<sup>23,24</sup> light-emitting polymers,<sup>25</sup> polymers bearing non-linear optics dyes,<sup>26</sup> and redox groups.<sup>27–31,33</sup> Tris(2,2'-bipyridine)ruthenium(II) and its derivatives are reported to have a relatively long lifetime of ca. 600 ns in the lowest excited triplet state<sup>12</sup> and to have a large rate constant of energy migration as high as  $10^8$ – $10^9 \text{ s}^{-1}$  in crystals<sup>34</sup> or in a polymer system.<sup>35</sup> Therefore, it is expected that efficient light-harvesting among Ru moieties is realized in well-defined thin films. However, there are no studies on energy migration among Ru moieties in layer-by-layer deposited films.

Here, we fabricated layer-by-layer deposited ultrathin films with polycations bearing Ru moieties and a polycation bearing ferrocene (Fc) moieties. To evaluate the diffusion coefficient of the energy migration in the Ru layers, we measured quenching of the phosphorescence of the Ru moiety by the Fc moiety and analyzed the quenching results with a one-dimensional diffusion equation. This study shows that the layer-by-layer films bearing the Ru moieties actually act as a light-harvesting layer in molecular assemblies.

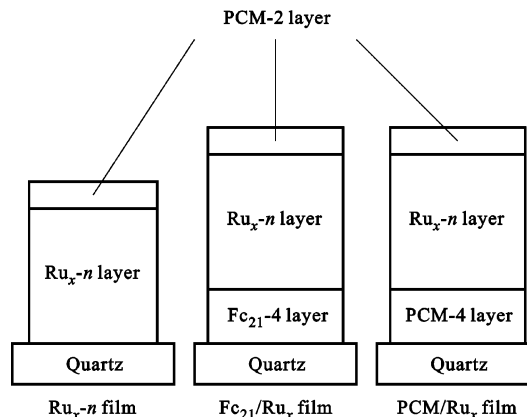
## Experimental Section

**Materials.** Chart 1 shows the chemical structures of the polycations used in this study. The polycation bearing the Fc moieties (P(CM-Fc<sub>21</sub>)) was synthesized as described elsewhere.<sup>30</sup> The molar fraction of the Fc moiety was 21%. The polycations (P(CM-Ru<sub>x</sub>)) bearing the Ru moieties where  $x$  denotes the

\* Address correspondence to this author. E-mail: sito@photo.polym.kyoto-u.ac.jp. Fax: +81-75-383-2617.

**CHART 1: Chemical Structures of P(CM-Ru<sub>x</sub>) and P(CM-Fc<sub>21</sub>)**

percentage of the Ru molar fraction in the copolymers ( $x = 4\%$ ,  $12\%$ , and  $18\%$ ) were synthesized as follows. 4-Hydroxy-methyl-4'-methyl-2,2'-bipyridine was synthesized from 4,4'-dimethyl-2,2'-bipyridine (Aldrich) by the method reported by Meyer et al.<sup>36</sup> 4-(Methacryloylmethyl)-4'-methyl-2,2'-bipyridine was obtained by a reaction between the product and methacryloyl chloride (Tokyo Kasei Co.) in the presence of triethylamine in chloroform at room temperature. The chloroform solution was washed several times with water whose pH was adjusted to be ca. 7 with K<sub>2</sub>CO<sub>3</sub>, and then dried over Na<sub>2</sub>SO<sub>4</sub>. Black oil obtained after evaporation of the chloroform solution was purified by column chromatography on silica gel. The eluent was a mixture of chloroform and methanol (v/v 98:2). A polycation bearing the bipyridyl moieties was obtained from the synthesized monomer and [2-(methacryloyloxy)ethyl]trimethylammonium chloride (Aldrich) by free radical copolymerization initiated by AIBN in degassed ethanol at 60 °C. The polycation was purified by reprecipitation from an ethanol solution into acetone several times. The copolymer P(CM-Ru<sub>x</sub>) was prepared by reflux of an ethanol solution with the polycation and *cis*-bis(2,2'-bipyridine)dichlororuthenium(II) hydrate (Aldrich). The copolymer P(CM-Ru<sub>x</sub>) was purified by reprecipitation from an ethanol solution into chloroform several times. The molar fraction of the Ru moiety in the copolymers was evaluated from the absorbance at 290 nm where tris(2,2'-bipyridine)dichlororuthenium(II) hexahydrate (Ru(bpy)<sub>3</sub>Cl<sub>2</sub>·6H<sub>2</sub>O) (Aldrich) has a molar absorption coefficient of  $8.07 \times 10^4 \text{ M}^{-1} \text{ cm}^{-1}$  in water. The density of the copolymer was evaluated to be 1.27 g cm<sup>-3</sup> for P(CM-Ru<sub>4</sub>), 1.31 g cm<sup>-3</sup> for P(CM-Ru<sub>12</sub>), and 1.36 g cm<sup>-3</sup> for P(CM-Ru<sub>18</sub>) from the buoyancy method with a mixture of chloroform and toluene. A polycation without the Ru moiety or the Fc moiety (PCM) was prepared by free radical polymerization of [2-(methacryloyloxy)ethyl]trimethylammonium chloride (Aldrich) in degassed ethanol at 60 °C. A polyanion, poly(acrylic acid) (PAA) ( $M_w = \text{ca. } 100\,000$ ), was purchased from Aldrich and used as received. Ferrocenemethanol prepared by a reduction of ferrocenecarboxaldehyde (Aldrich) by sodium borohydride (Nacalai Tesque) and Ru(bpy)<sub>3</sub>Cl<sub>2</sub> were used as model compounds for the Fc moiety and the Ru moiety in the polycations, respectively. Quartz substrates were immersed into a Piranha solution overnight, and then rinsed with ultrapure water. Ultrapure water used for the layer-by-layer deposition was prepared by deionization, distillation, and then passing through a filtration system (Barnstead Nanopure II).

**CHART 2: Schematic Illustrations of the Layer Structures Used in This Study**

**Preparation of Layer-by-Layer Ultrathin Film.** Layer-by-layer films were prepared by repetitive cycles of immersion of the quartz substrates into solutions in the following order: an aqueous solution of P(CM-Fc<sub>21</sub>) or P(CM-Ru<sub>x</sub>) with a concentration of 10 mM for 5 min, water for 3 min, an aqueous solution of PAA with a concentration of 10 mM for 5 min, and water for 3 min. The concentrations are based on the molecular weight of their monomer units. The PAA solution was adjusted to be pH 6.5 with sodium hydroxide. The substrates were dried in the air for 3 min after each immersion. The procedure described above was performed under a relative humidity of 50–60%. Hereafter, we will use the abbreviation “Ru<sub>x-n</sub>”, which refers to a layer-by-layer film consisting of  $n$  bilayers of P(CM-Ru<sub>x</sub>) and PAA. Another abbreviation “Fc<sub>21</sub>/Ru<sub>x</sub>” refers to a heterostructured layer-by-layer film prepared by sequential deposition of a Ru<sub>x-n</sub> film on a 5-nm Fc film consisting of four bilayers of P(CM-Fc<sub>21</sub>) and PAA. The characterization of the Fc layer is described elsewhere.<sup>30</sup> Two bilayers of PCM and PAA were further deposited as an overcoat layer. Chart 2 illustrates the layer structures used in this study.

**Measurements.** Absorption and emission spectra were measured with a spectrophotometer (Hitachi, U-3500) and a fluorescence spectrophotometer (Hitachi, F-4500), respectively. Excitation wavelength was 460 nm. Phosphorescence decay of the Ru moiety in layer-by-layer films was measured by transient emission spectroscopy. A picosecond laser pulse at 355 nm from a Nd:YAG laser (EKSPLA, PL2400B) was used as an excitation light source. The power of the laser pulse was attenuated with stainless-wire mesh filters to avoid triplet–triplet annihilation. The phosphorescence from the films was detected with a photomultiplier tube (Hamamatsu Photonics, R1477) after passing through a monochromator (Ritsh, MC-10N) set at 600 nm with a cut filter (L-37) for the excitation light. The emission signal decay was analyzed with a digital oscilloscope (Tektronics, TDS3032B).

## Results and Discussion

**Preparation and Characterization of the Layer-by-Layer Films Bearing the Ru Moieties.** Figure 1 shows the absorption spectra of Ru<sub>18-n</sub> ( $n = 2, 4, 6, 8$ ) films on quartz substrates. The absorption spectra were similar to that of Ru(bpy)<sub>3</sub>Cl<sub>2</sub> in water. These absorption peaks at 290 and 460 nm were ascribed to the ligand centered  $\pi \rightarrow \pi^*$  and the metal to ligand charge transfer  $d \rightarrow \pi^*$  transitions of the Ru moiety.<sup>12</sup> This shows that the Ru moieties are introduced in the films without a significant change in their electronic state. The absorbance at 290 nm

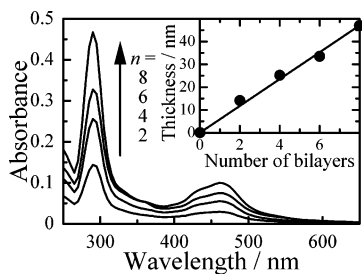


**Figure 1.** Absorption spectra of  $\text{Ru}_{18-n}$  ( $n = 2, 4, 6, 8$ ) films on quartz substrates. The inset shows the relationship between the number of bilayers and the thickness evaluated from the absorbance at 290 nm.

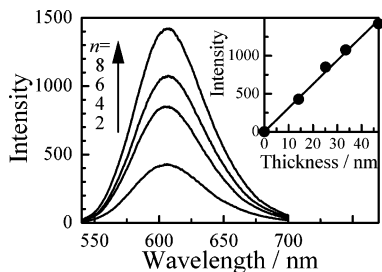


**Figure 2.** Emission spectra of  $\text{Ru}_{18-n}$  ( $n = 2, 4, 6, 8$ ) at room temperature. The inset shows the relationship between the thickness and the intensity of the phosphorescence at 605 nm. The experimental error was within the radius of the circles.

increased linearly as the number of bilayers increased. The inset in Figure 1 shows the relationship of the number of bilayers and the thickness of the films. The thickness per bilayer was evaluated to be ca. 6 nm from the absorbance at 290 nm, using a molar absorption coefficient of  $8.07 \times 10^4 \text{ M}^{-1} \text{ cm}^{-1}$ , a density of  $1.36 \text{ g cm}^{-3}$  for the bilayer, and a Ru molar fraction of 0.18. The linear increase shows the steady growth of the multilayered film in a scale of nanometers with the increase in the number of bilayers. Similarly, steady growth was observed in the absorption spectra of  $\text{Ru}_4$  and  $\text{Ru}_{12}$  layer-by-layer films. The thickness per bilayer is controllable in a range of ca. 2 to 6 nm by changing the deposition conditions such as drying time. These results show that ultrathin polymer films bearing the Ru moieties are fabricated by the layer-by-layer deposition technique. In this study, the thickness per bilayer was adjusted to be ca. 2 nm for  $\text{Ru}_4$  films and ca. 6 nm for  $\text{Ru}_{12}$  and  $\text{Ru}_{18}$  films.

Figure 2 shows the emission spectra of  $\text{Ru}_{18-n}$  ( $n = 2, 4, 6, 8$ ) films at room temperature. All the films showed a broad emission band around 605 nm. This emission band was ascribed to the phosphorescence of the Ru moiety in the films.<sup>12</sup> The inset shows the relationship between the thickness and the intensity of the phosphorescence at 605 nm. The experimental error was within the radius of the circles. The intensity was proportional to the thickness of the films. This linearity is also consistent with the steady growth as shown in the absorption spectra of the films. The lifetime of the phosphorescence was evaluated from the decay curve of the phosphorescence. The decay curves were well fitted with a sum of two exponential functions, where  $I_0(t)$  is the intensity of the phosphorescence at time  $t$ .

$$I_0(t) = I_0(0) \left\{ A \exp\left(-\frac{t}{\tau_1}\right) + (1 - A) \exp\left(-\frac{t}{\tau_2}\right) \right\} \quad (1)$$

The average lifetime  $\langle\tau\rangle$  was calculated as follows.

$$\langle\tau\rangle = A\tau_1 + (1 - A)\tau_2 \quad (2)$$

**TABLE 1: Fitting Parameters in Eq 1 for a  $\text{PCM/Ru}_4$  Film, a  $\text{PCM/Ru}_{12}$  Film, and a  $\text{PCM/Ru}_{18}$  Film**

	$A^a$	$\tau_1/\text{ns}^a$	$\tau_2/\text{ns}^a$	$\langle\tau\rangle/\text{ns}$
$\text{PCM/Ru}_4$	0.55	710	130	$450 \pm 50$
$\text{PCM/Ru}_{12}$	0.44	580	98	$310 \pm 30$
$\text{PCM/Ru}_{18}$	0.44	620	100	$330 \pm 30$

<sup>a</sup> The experimental error was within 5%.

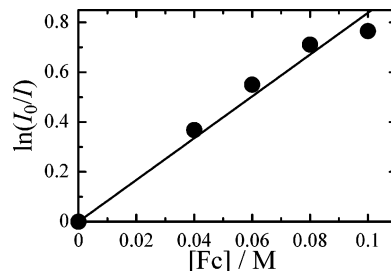


**Figure 3.** Perrin plots for the quenching of the phosphorescence of  $\text{Ru}(\text{bpy})_3\text{Cl}_2$  in PCM spincast films containing ferrocenemethanol at various concentrations.

The experimental error of  $\tau_1$  and  $\tau_2$  was 5% at most. The fitting parameters and  $\langle\tau\rangle$  are listed in Table 1. We will discuss triplet energy migration in the layer-by-layer films in the next section.

**Energy Migration in the Layer-by-Layer Films.** First, we evaluated the quenching radius of the Fc moiety for the Ru moiety in the lowest excited triplet state. Figure 3 shows the Perrin plots for the quenching of the phosphorescence of  $\text{Ru}(\text{bpy})_3\text{Cl}_2$  in PCM spincast films containing ferrocenemethanol at various concentrations. As shown in Figure 3, a linear relationship was observed over a wide concentration range. Energy migration of the excited Ru molecules in the film is negligible because the concentration of the Ru molecules is as low as 5 mM that each Ru molecule is considered to be isolated. The quenching radius was evaluated to be 1.5 nm from the slope. A Förster radius for the dipole–dipole interaction between the Ru moiety and the Fc moiety was as short as 0.5 nm because of little spectral overlap of the absorption spectrum of the Fc moiety and the emission spectrum of the Ru moiety. Thus, the quenching mechanism is not due to Förster-type energy transfer but due to electron transfer or Dexter-type energy transfer. Since the latter two mechanisms require overlap of the molecular orbitals, the quenching rate falls off exponentially with an increase in the separation distance. Therefore, it can be safely said that the Perrin model is a good approximation for the quenching of the Ru moiety by the Fc moiety.

Next, we discuss the quenching in heterostructured layer-by-layer films. The solid lines in parts a, b, and c of Figure 4 show the emission spectra of a  $\text{Fc}_{21}/\text{Ru}_4$  film, a  $\text{Fc}_{21}/\text{Ru}_{12}$  film, and a  $\text{Fc}_{21}/\text{Ru}_{18}$  film, respectively. The broken lines in the figure show the emission spectra of a  $\text{PCM/Ru}_4$  film, a  $\text{PCM/Ru}_{12}$  film, and a  $\text{PCM/Ru}_{18}$  film, respectively, as the references. The thickness of the Ru layers and the Fc layer was ca. 15 and 5 nm, respectively. The intensity was normalized by that of the corresponding reference at 605 nm. The normalized intensity was smaller than that of the corresponding reference and decreased with the increase in the concentration of the Ru moiety. For the  $\text{Fc}_{21}/\text{Ru}_4$  film, the normalized intensity was ca. 0.85. The concentration of the Ru moiety in the  $\text{Ru}_4$  film is so low that each Ru moiety is considered to be isolated. Assuming that only the Ru moieties within the Perrin radius are quenched, the emission efficiency is calculated to be 0.90 because the radius and the total thickness of the Ru layer are 1.5 and 15 nm, respectively. The value of the emission efficiency is in good

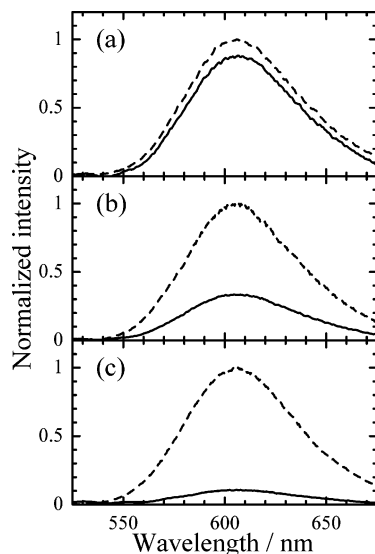


**Figure 4.** Emission spectra of  $\text{Fc}_{21}/\text{Ru}_x$  films (solid lines) and  $\text{PCM}/\text{Ru}_x$  films (broken lines) ((a)  $x = 4$ , (b)  $x = 12$ , and (c)  $x = 18$ ). The  $\text{Ru}_x$  layers and the  $\text{Fc}_{21}$  layer had a thickness of ca. 15 and 5 nm, respectively. The intensity was normalized by that of the corresponding reference at 605 nm.

agreement with the value of normalized intensity. In other words, there is no energy migration among the Ru moieties in the  $\text{Fc}_{21}/\text{Ru}_4$  film. For the  $\text{Fc}_{21}/\text{Ru}_{12}$  film, on the other hand, the normalized intensity was 0.33, which is much smaller than that of the  $\text{Fc}_{21}/\text{Ru}_4$  film. This small value shows that the quenching takes place not only at the interface but also in the bulk of the Ru layer. For the  $\text{Fc}_{21}/\text{Ru}_{18}$  film, the normalized intensity was as small as 0.11, showing that almost all Ru moieties were quenched. These results show that there exists efficient energy migration among the Ru moieties at the high concentrations of the Ru moiety. Even if a  $\text{Ru}^*$  moiety in the excited state is formed far from the Fc layer, it can reach the Fc layer by the energy migration. It should be noted that the normalized intensity of the  $\text{Fc}_{21}/\text{Ru}_4$  film, where the energy migration is negligible, gives information on the structure of the films. The agreement of the normalized intensity with the calculated one indicates that interpenetration of polymer chains in the films, which is always seen in layer-by-layer films,<sup>19</sup> can be ignored. If the Ru and the Fc layers were mixed significantly, the normalized intensity would be smaller than that observed.

The dependence of the intensity of the phosphorescence at 605 nm on the thickness of the Ru layers was examined to analyze the energy migration quantitatively. The dependence is shown in Figure 5a–c. The closed circles in the figures stand for the intensity of the phosphorescence of  $\text{Fc}_{21}/\text{Ru}_4$ ,  $\text{Fc}_{21}/\text{Ru}_{12}$ , and  $\text{Fc}_{21}/\text{Ru}_{18}$  films with various thicknesses of the Ru layers, respectively. The open circles in the figures stand for the intensity of the phosphorescence of  $\text{PCM}/\text{Ru}_4$ ,  $\text{PCM}/\text{Ru}_{12}$ , and  $\text{PCM}/\text{Ru}_{18}$  films with various thicknesses of the Ru layers, respectively, which were used as the references. The solid curves show the theoretical calculation based on diffusion of the excitation energy, which will be discussed later. The experimental error was within the radius of the circles. The intensity of the references in the figures, as drawn by the broken lines, was proportional to the thickness of the Ru layers. The difference in the intensity between the solid line and the broken curve at a given thickness corresponds to the number of quenched Ru moieties. As seen in Figures 4 and 5, the quenching was more efficient as the concentration of the Ru moiety in the films increased. This dependence on the concentration shows that the

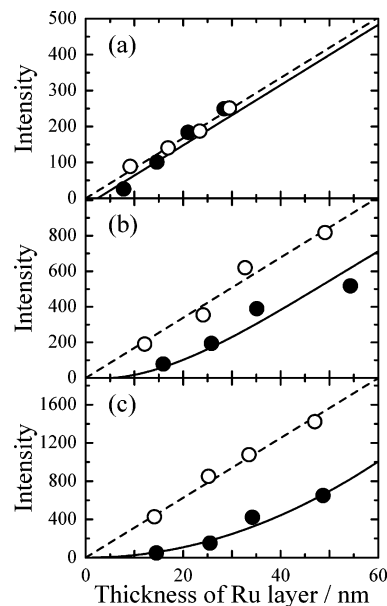
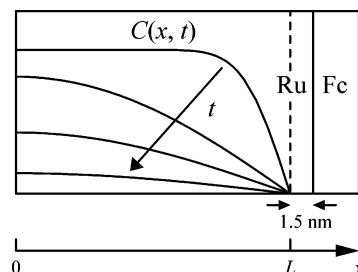


**Figure 5.** Dependence of the intensity of the phosphorescence at 605 nm on the thickness of the Ru layers in (a)  $\text{Fc}_{21}/\text{Ru}_4$  (closed circles) and  $\text{PCM}/\text{Ru}_4$  (open circles) films, in (b)  $\text{Fc}_{21}/\text{Ru}_{12}$  (closed circles) and  $\text{PCM}/\text{Ru}_{12}$  (open circles) films, and in (c)  $\text{Fc}_{21}/\text{Ru}_{18}$  (closed circles) and  $\text{PCM}/\text{Ru}_{18}$  (open circles) films. The solid lines are theoretical fits for evaluation of the diffusion coefficient of the energy migration. The experimental error was within the radius of the circles.

#### SCHEME 1: Time Evolution of the Concentration Profile for the $\text{Ru}^*$ Moiety in the Excited State in the Heterostructured Films



excitation energy migrates among the Ru moieties. For the  $\text{Fc}_{21}/\text{Ru}_4$  films, the difference was independent of the thickness of the films, indicating that the quenching occurs only at the interface. This shows that the energy migration in  $\text{Fc}_{21}/\text{Ru}_4$  films is negligible. For  $\text{Fc}_{21}/\text{Ru}_{12}$  and  $\text{Fc}_{21}/\text{Ru}_{18}$  films, on the other hand, the difference increased as the thickness of the films increased, indicating that the distance of the energy migration is comparable with the thickness of the films used in this study. It should be noted that the phosphorescence intensity of the reference  $\text{PCM}/\text{Ru}_x$  films at a given thickness was proportional to the molar concentration of the Ru moiety in the films. This linearity is consistent with the decay kinetics of the excited Ru moiety that was almost independent of the molar fraction of the Ru moiety. This may be attributed to the homogeneous distribution of the Ru moieties in the polymer films.<sup>37,38</sup>

The amount of the excitation energy transported to the interface is determined by the diffusion coefficient  $D$  of the excitation energy and the lifetime of the  $\text{Ru}^*$  moiety in the excited state. Here, we used a one-dimensional diffusion model shown in Scheme 1 to evaluate  $D$  in the Ru layers. We define an  $x$ -axis in the direction normal to the layer plane and set the origin to the interface between the Ru layer and the air. The thickness of the Ru layer is  $L + 1.5$  nm (the Perrin radius). The concentration  $C(x, t)$  of the  $\text{Ru}^*$  moiety in the excited state



at location  $x$  and at time  $t$  obeys Fick's law of diffusion.

$$\frac{\partial C(x,t)}{\partial t} = D \frac{\partial^2 C(x,t)}{\partial x^2} \quad (3)$$

Excitation at  $t = 0$  makes the concentration of the Ru\* moiety in the excited state  $C_0$  everywhere in the film because the absorbance of the film was less than 0.1, which is small enough to excite the film homogeneously. Therefore, the initial condition is as follows.

$$C(x,0) = C_0 \quad (4)$$

The phosphorescence intensity can be calculated as the integral of the decay curve of the phosphorescence over the whole time range from  $t = 0$  to infinity,

$$I_{\text{total}} = \int_0^\infty I_0(t) \int_0^L C(x,t) dx dt \quad (5)$$

where  $I_0(t)$  is the decay curve of the phosphorescence in the absence of the quenching wall, which can be given by eq 1 with the fitting parameters listed in Table 1. The concentration of the Ru\* moiety in the excited state at  $x = L$  is always 0 because of the quenching by the Fc layer. Therefore, one of the boundary conditions is as follows.

$$C(L,t) = 0 \quad (6)$$

The film is not thick enough to regard as infinite because the excitation energy can migrate throughout the film as discussed above. The other boundary condition for the finite diffusion shown in Scheme 1 is as follows.<sup>39</sup>

$$\left[ \frac{\partial C(x,t)}{\partial x} \right]_{x=0} = 0 \quad (7)$$

Equation 3 can be solved under the boundary and the initial conditions.<sup>39</sup>

$$C(x,t) = C_0 - C_0 \sum_{n=0}^{\infty} (-1)^n \left[ \operatorname{erfc} \left\{ \frac{(2n+1)L-x}{2\sqrt{Dt}} \right\} + \operatorname{erfc} \left\{ \frac{(2n+1)L+x}{2\sqrt{Dt}} \right\} \right] \quad (8)$$

As seen in Figure 5, the theoretical fits shown by the solid lines agreed well with the experimental data. The diffusion coefficient obtained was  $<1 \times 10^{-7} \text{ cm}^2 \text{ s}^{-1}$  in the Ru<sub>4</sub> layers,  $7 \times 10^{-6} \text{ cm}^2 \text{ s}^{-1}$  in the Ru<sub>12</sub> layers, and  $2 \times 10^{-5} \text{ cm}^2 \text{ s}^{-1}$  in the Ru<sub>18</sub> layers. The root mean square of migration distance  $\langle x^2 \rangle^{1/2}$  in the lifetime of the Ru\* moiety in the excited triplet state  $\langle \tau \rangle$  was calculated by  $\langle x^2 \rangle^{1/2} = (2D \langle \tau \rangle)^{1/2}$ .<sup>40</sup> The value in Ru<sub>18</sub> layers was 36 nm, which is much longer than the Perrin radius of 1.5 nm, and as long as that of the singlet excitation energy in an excimer-free cast film of a homopolymer bearing carbazole moieties,<sup>14</sup> and only one order shorter than those of singlet excitation energy even in crystals of aromatic hydrocarbons.<sup>40</sup> Although the triplet excitation energy of the Ru\* moiety has a smaller diffusion coefficient than the singlet excitation energy, the excited triplet state of Ru\* has a much longer lifetime than the singlet excited state of aromatic hydrocarbons. This is one of the reasons for the efficient triplet energy migration among

the Ru moieties. The efficient migration shows that the layer-by-layer films serve as a light-harvesting system.

## Conclusions

Ultrathin polymer films bearing the Ru moieties at various concentrations were fabricated by the layer-by-layer deposition technique. The absorption and the emission spectra were similar to those of Ru(bpy)<sub>3</sub>Cl<sub>2</sub>. This similarity shows that the Ru moieties are introduced into the films without significant change in their electronic state. The phosphorescence of the Ru moiety was quenched by the Fc moiety via energy migration among the Ru moieties. The distance of the energy migration strongly depended on the concentration of the Ru moiety. The diffusion coefficient for the energy migration was evaluated to be  $<1 \times 10^{-7}$ ,  $7 \times 10^{-6}$ , and  $2 \times 10^{-5} \text{ cm}^2 \text{ s}^{-1}$  in the Ru<sub>4</sub>, the Ru<sub>12</sub>, and the Ru<sub>18</sub> layers, respectively. The root mean square of the migration distance in the Ru<sub>18</sub> layers was calculated to be 36 nm, which is much longer than the Perrin radius for the quenching of the Ru moiety by the Fc moiety, and as long as or only one order shorter than those of singlet excitation energy. This study shows that the layer-by-layer films bearing the Ru moieties serve as a light-harvesting layer in molecular assemblies.

**Acknowledgment.** This work was supported by the Integrative Industry–Academia Partnership (IIAP) including Kyoto University, Nippon Telegraph and Telephone Corporation, Pioneer Corporation, Hitachi, Ltd., Mitsubishi Chemical Corporation, and Rohm Co., Ltd.

## References and Notes

- (1) Kuhn, H. *J. Photochem.* **1979**, *10*, 111–132.
- (2) Möbius, D. *Acc. Chem. Res.* **1981**, *14*, 63–68.
- (3) Fujihira, M.; Nishiyama, K.; Yamada, H. *Thin Solid Films* **1985**, *132*, 77–82.
- (4) Ohmori, S.; Ito, S.; Yamamoto, M. *Macromolecules* **1991**, *24*, 2377–2384.
- (5) Ohkita, H.; Ishii, H.; Ito, S.; Yamamoto, M. *Chem. Lett.* **2000**, 1092–1093.
- (6) Ohkita, H.; Ishii, H.; Ogi, T.; Ito, S.; Yamamoto, M. *Radiat. Phys. Chem.* **2001**, *60*, 427–432.
- (7) Ohkita, H.; Ogi, T.; Kinoshita, R.; Ito, S.; Yamamoto, M. *Polymer* **2002**, *43*, 3571–3577.
- (8) Aoki, A.; Abe, Y.; Miyashita, T. *Langmuir* **1999**, *15*, 1463–1469.
- (9) Taniguchi, T.; Fukasawa, Y.; Miyashita, T. *J. Phys. Chem. B* **1999**, *103*, 1920–1924.
- (10) Terasaki, N.; Akiyama, T.; Yamada, S. *Langmuir* **2002**, *18*, 8666–8671.
- (11) Yamada, H.; Imahori, H.; Nishimura, Y.; Yamazaki, I.; Ahn, T. Y.; Kim, S. K.; Kim, D.; Fukuzumi, S. *J. Am. Chem. Soc.* **2003**, *125*, 9129–9139.
- (12) Juris, A.; Balzani, V.; Barigelli, F.; Campagna, S.; Belser, P.; von Zelewsky, A. *Coord. Chem. Rev.* **1988**, *84*, 85–277.
- (13) Nazeeruddin, M. K.; Kay, A.; Rodicio, I.; Humphry-Baker, R.; Müller, E.; Liska, P.; Vlachopoulos, N.; Grätzel, M. *J. Am. Chem. Soc.* **1993**, *115*, 6382–6390.
- (14) Ohmori, S.; Ito, S.; Yamamoto, M. *Ber. Bunsen-Ges. Phys. Chem.* **1989**, *93*, 815–824.
- (15) Hisada, K.; Ito, S.; Yamamoto, M. *Langmuir* **1996**, *12*, 3682–3687.
- (16) Hisada, K.; Ito, S.; Yamamoto, M. *J. Phys. Chem. B* **1997**, *101*, 6827–6833.
- (17) Kerp, H. R.; Donker, H.; Koehorst, R. B. M.; Schaafsma, T. J.; van Faassen, E. E. *Chem. Phys. Lett.* **1998**, *298*, 302–308.
- (18) Decher, G.; Hong, J. D. *Makromol. Chem. Macromol. Symp.* **1991**, *46*, 321–327.
- (19) Decher, G. *Science* **1997**, *277*, 1232–1237.
- (20) Shimazaki, Y.; Mitsuishi, M.; Ito, S.; Yamamoto, M. *Langmuir* **1998**, *14*, 2768–2773.
- (21) Shimazaki, Y.; Mitsuishi, M.; Ito, S.; Yamamoto, M.; Inaki, Y. *Thin Solid Films* **1998**, *333*, 5–8.
- (22) Shimazaki, Y.; Nakamura, R.; Ito, S.; Yamamoto, M. *Langmuir* **2001**, *17*, 953–956.

- (23) Stockton, W. B.; Rubner, M. F. *Macromolecules* **1997**, *30*, 2717–2725.
- (24) Ram, M. K.; Salerno, M.; Adami, M.; Faraci, P.; Nicolini, C. *Langmuir* **1999**, *15*, 1252–1259.
- (25) Baur, J. W.; Rubner, M. F.; Reynolds, J. R.; Kims, S. *Langmuir* **1999**, *15*, 6460–6469.
- (26) Shimazaki, Y.; Ito, S.; Tsutsumi, N. *Langmuir* **2000**, *16*, 9478–9482.
- (27) Laurent, D.; Schlenoff, J. B. *Langmuir* **1997**, *13*, 1552–1557.
- (28) Hodak, J.; Etchenique, R.; Calvo, E. J.; Singhal, K.; Bartlett, P. N. *Langmuir* **1997**, *13*, 2708–2716.
- (29) Wu, A.; Yoo, D.; Lee, J.-K.; Rubner, M. F. *J. Am. Chem. Soc.* **1999**, *121*, 4883–4891.
- (30) Fushimi, T.; Oda, A.; Ohkita, H.; Ito, S. *Thin Solid Films*. Submitted for publication.
- (31) Kaschak, D. M.; Johnson, S. A.; Waraksa, C. C.; Pogue, J.; Mallouk, T. E. *Cood. Chem. Rev.* **1999**, *185–186*, 403–416.
- (32) Kumaraswamy, G.; Dibaj, A. M.; Caruso, F. *Langmuir* **2002**, *18*, 4150–4154.
- (33) Grant, P. S.; McShane, M. J. *IEEE Sensors J.* **2003**, *3*, 139–146.
- (34) Ikeda, N.; Yoshimura, A.; Tsushima, M.; Ohno, T. *J. Phys. Chem. A* **2000**, *104*, 6158–6164.
- (35) Fleming, C. N.; Maxwell, K. A.; DeSimone, J. M.; Meyer, T. J.; Papanikolas, J. M. *J. Am. Chem. Soc.* **2001**, *123*, 10336–10347.
- (36) Ciana, L. D.; Hamachi, I.; Meyer, T. J. *J. Org. Chem.* **1989**, *54*, 1731–1735.
- (37) Rudmann, H.; Shimada, S.; Rubner, M. F. *J. Am. Chem. Soc.* **2002**, *124*, 4918–4921.
- (38) Bernhard, S.; Barron, J. A.; Houston, P. L.; Abruña, H. D.; Ruglovksy, J. L.; Gao, X.; Malliaras, G. G. *J. Am. Chem. Soc.* **2002**, *124*, 13624–13628.
- (39) Oglesby, D. M.; Omang, S. H.; Reilley, C. N. *Anal. Chem.* **1965**, *37*, 1312–1316.
- (40) Birks, J. B. *Photophysics of Aromatics Molecules*; Wiley-Interscience: London, UK, 1970; Chapter 11.